Proceedings of the Research Institute of Atmospherics,
Nagoya University, vol. 21 (1974)

THE ESTIMATION OF WHISTLER PATH LATITUDE FROM THE NOSE EFFECT OF LOW LATITUDE WHISTLERS

Mizuo KASHIWAGI

Abstract

Some results of estimation of whistler path latitude from the nose effect of whistlers observed at Moshiri (geom. lat. 34°) are described. In the calculation of dispersion, we have adopted the gyrofrequency model and exponential one for the magnetospheric electron density profile. First, the observed dispersion in the routine-base observation is utilized to determine the factors specifying the models such as density gradient etc. for varying path latitudes. The nose effect is calculated for such models and is compared with the observation. Then the path latitude is determined such that the observed nose effect is closed to the calculation. And it is found that the path latitude determined for the exponential model is closer to the latitude derived from the experimental formula by Allcock.

At high latitudes the estimation of whistler path latitude, which is a field aligned path intersecting at the Earth's surface, is easily and accurately made by using the nose frequency of whistlers, because the nose frequency shows slight dependence on the distribution model of electron density along the propagation path. Whilst, at low latitudes such an estimation becomes more difficult because of the close relation of the nose frequency with the electron density model. Moreover, at low latitudes such as Moshiri the nose frequency becomes higher than several tens of kHz, so that no nose whistler is detectable because of the strong ionospheric absorption except in a few fortunate cases (Ohtsu, 1967). Even the reception is, practically, difficult of the whistlers displaying the nose effect that the frequency versus time curve deviates from the f−t curve given by the Eckersley's law in the higher frequency above 10kHz.

During the special observation period for nose whistlers made in winter season of 1971 at Moshiri, some whistlers of which the frequency range extended up to 30kHz were observed. An example of the sonagram of whistlers observed at 18:32 J. S. T. on March 1971 is shown in Fig. 1. Fig. 1(a) shows a whistler in the low frequency range below 8kHz obtained from the routine observation. Fig. 1(b) represents the higher frequency portion of the same whistler. The f−t curve (B) based on the Eckersley's law is inscribed in Fig. 1(b). As seen in this figure, the deviation from the calculated dispersion curve becomes greater as the frequency increases. The nose effect begins to appear at about 10kHz and it is clearly confirmable at 30kHz.

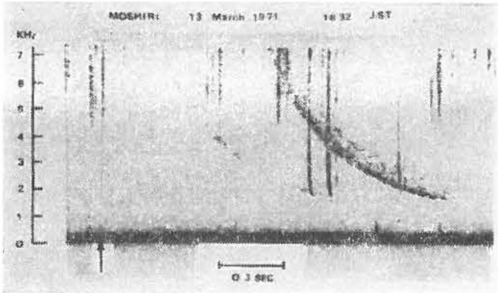

Fig. 1 a The low frequency portion of whistlers based on routine observations.

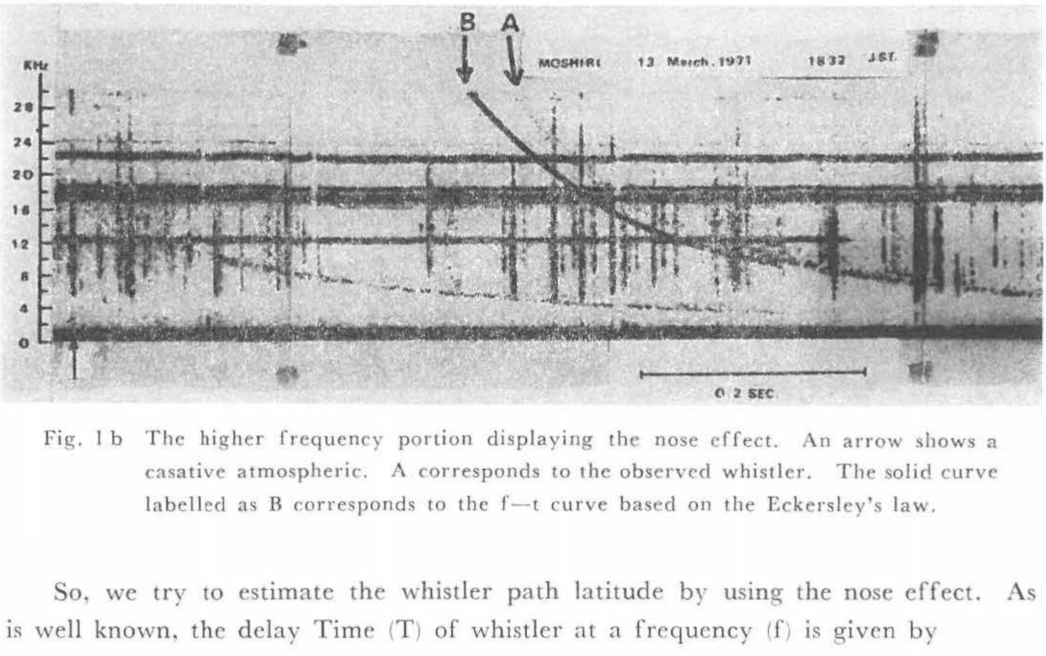

Fig. 1 b The higher frequency portion displaying the nose effect. An arrow shows a casative atmospheric. A corresponds to the observed whistler. The solid curve labelled as B corresponds to the f—t curve based on the Eckersley's law.

So, we try to estimate the whistler path latitude by using the nose effect. As is well known, the delay Time (T) of whistler at a frequency (f) is given by

$$T = \frac{1}{2C} \int_{path} \frac{f_0 \, f_H \, ds}{f^{1/2} (f_H - f)^{3/2}}$$

where, C is light velocity, f_0 is plasma frequency, f_H is gyrofrequency and ds is the element of path length. Hence, the dispersion (D) is given by

$$D = \frac{1}{2C} \int_{path} \frac{f_0 \, f_H \, ds}{(f_H - f)^{3/2}}$$

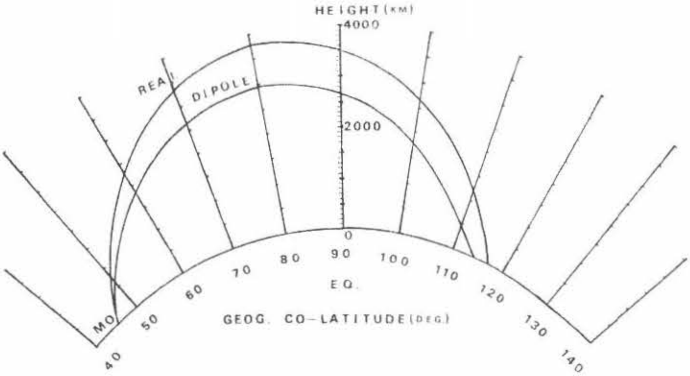

Fig. 2 The centered dipole field line and the geomagnetic field line calculated with the higher harmonic series of 5 orders.

At low latitudes the centered dipole field is different from the real magnetic field of the Earth. Therefore, we adopted the geomagnetic field model improved by Cain and Sweeney (1970) for the calculation of the time delay and dispersion. The calculated field line with the harmonic series of 5 orders and the centered dipole field line starting at Moshiri are demonstratively illustrated in Fig. 2. For the distribution models of electron density along a field line, we adopt the gyrofrequency model and the exponential one. The adopted gyrofrequency model consists of three regions. In the Region I from 100km to the height of F2 maximum, the electron density being null at 100km increases parabolically with height.

The F2 maximum height (r_m) is assumed to be the virtual height of F layer (h'F). In the Region II from F2 maximum height to the upper boundary (r_2), the electron density is followed by a Chapman distribution with the scale height of 100km. In Region III, the electron density is proportional to the gyrofrequency. Then, the electron density profile in each region is expressed as follows.

Region I

$$N = Nm\left[1-\left(\frac{r}{r_m-100}\right)^2\right] \qquad \text{for } r_m \geq r \geq 100\text{km}$$

where, $Nm = 1.24 \times (f_0 F2)^2 \times 10^{-8}/\text{cm}^3$.

Region II

$$N = Nm \exp\left[\frac{1}{2}\left[\left(1-\frac{r-r_m}{100}\right) - \exp\left(-\frac{r-r_m}{100}\right)\right]\right] \quad \text{for } r_2 \geq r \geq r_m$$

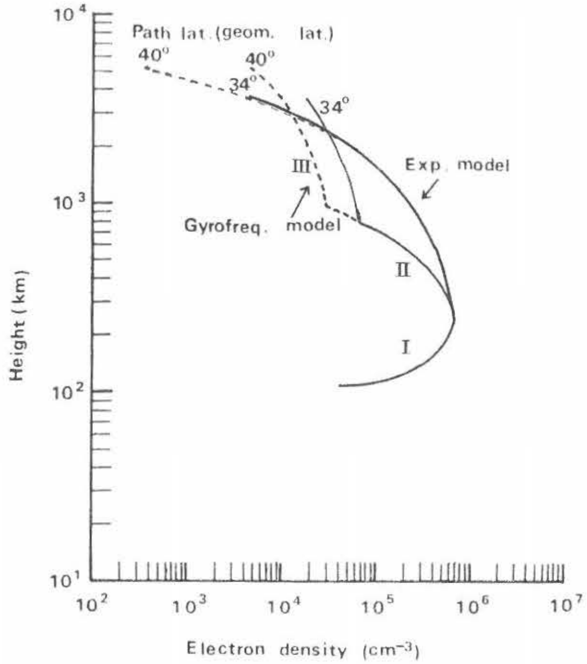

Fig. 3 Examples of electron density distributions along the magnetic field lines.

Region III

$$N \propto N_{2m} \times f_H \qquad \text{for} \quad r \geq r_2$$

where N_{2m} is electron density at r_2. The height (r_2) of upper boundary of the Region II is determined by maching the calculated dispersion value without the nose effect along a geomagnetic field line with the observed dispersion value at 2kHz. Secondly, we consider the case of the exponential model. Similarly at the case of the gyrofrequency model, the electron density increases parabolically below F2 maximum height. Above F2 maximum height the density decreases with increasing height as in the form.

$$N = Nm \exp[-k(r-r_m)]$$

where, k is the gradient determind by matching the calculated dispersion value with the observed one at 2kHz. The calculation of electron densities is carried out in one degree step along the field lines terminating at the Earth's surface from geomagnetic

J. S. T.	Akita geom. lat. 29.5°	30°	31°	32°	33°	34°	35°	Wakkanai 35.5°	36°
18h 00m	f_0F2 7.6 MHz h′F 235 km							8.0 225	
18h 32m	f_0 F2 h′ F	7.0 233	7.0 233	7.2 233	7.3 234	7.5 234	7.6 234		7.6 234
19h 00m	f_0F2 5.9 MHz h′F 230 km							7.2 245	

Table 1 The values of f_0F2 and h′F obtained by the interpolation method.

latitude 30° to 44°. The values of f_0F2 and h′F in the relevant time and latitude are estimated by interpolating the values at Akita (geom. lat. 29.5°) and Wakkanai (35.5°). At higher latitudes than 36°, the ionospheric values at Wakkanai are used. The interpolated f_0F2 and h′F values are given in Table 1. A few examples of the results obtained on the electron densities are presented in Fig. 3.

The ratio [D(f)/Do] of the dispersion [D(f)] at a frequency of f kHz to the observed dispersion value at 2kHz (Do), which is indicated ‘the nose effect’, is calculated along the field line starting at the Earth's surface from 30° to 44° for the gyrofrequency model and the exponential one.

The similar ratio obtained on whistler data are compared with the calculated

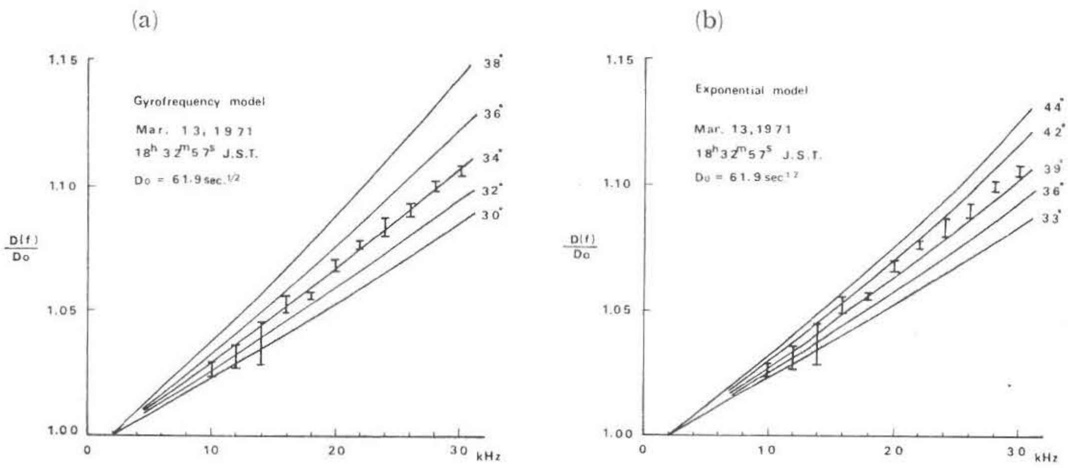

Fig. 4 Ratio of the dispersion at a frequency of f kHz to the dispersion at 2kHz, versus frequency. Solid curves correspond to the ratios for the dispersions calculated along the geomagnetic field lines intersecting at the Earth's surface in the geomagnetic latitude from 30° to 44°. Vertical dashed lines correspond to the ratios for the observed dispersions.

(a) for the gyrofrequecy model.

(b) for the exponential model.

March 13, 1971 Moshiri			
J. S. T.	Do (sec.)	Gyrofreq. model (geom. lat.)	Exp. model (geom. lat.)
18h 30m 30s	62.1	32° — 34°	38° — 41°
18h 32m 57s	61.9	33° — 35°	39° — 42°
18h 34m 13s	62.1	34° — 35°	39° — 42°
18h 34m 49s	62.3	34° — 35°	39° — 42°
18h 58m 04s	62.0	32° — 34°	37° — 40°
19h 14m 31s	61.4	33° — 34°	38° — 41°

Table 2 The estimated whistler path latitudes for the gyrofrequency and exponential models.

one. Then, the latitude where the observed ratio is best fitted to the calculated one is chosen to be the whistler path latitude. Examples on the ratios [D(f)/Do] are illustrated in Fig. 4. Solid curves correspond to the ratios for the calculated dispersion. Vertical dashed lines correspond to the same ratios for the observed dispersion. The error bar is the consequence of the diffuseness of whistler. It is found from the figure that the path latitude is in the range from 33° to 35° for the gyrofrequency model and from 39° to 42° for the exponential model. The path latitudes obtained by using the nose effect are summarized in Table 2.

Allcock (1959) represents the experimental formula of the dispersion (D) versus geomagnetic latitude (θ) given by $D \simeq 2.2\ (\theta - 12)$, so that the path latitude is 39° of whistler with the dispersion of 60 sec.$^{1/2}$. The path latitude is also found to be about 40° for the calculated dispersion of 60 sec.$^{1/2}$ by using the topside ionospheric electron density data measured by Alouett 2 satellite over Japan (Tanaka). Judging from these results, the simple estimation of the whistler path latitude can be done by using the exponential model. But at low latitudes the use of nose effect for the decision of the path latitude may be thought to be difficult considering that the higher frequency component of whistlers is not detectable and the accuracy is worse at higher frequency as a consequence of the diffuseness of whistler even if the higher frequency component is received.

Acknowledgement

The author wishes to express his sincere thanks to Profs. A. Iwai, J. Ohtsu, T. Kamada and Dr. Y. Tanaka of the Research Institute of Atmospherics of Nagoya University for their kind guidance and advice.

References

Allcock, G. Mck.: The electron density distribution in the outer ionosphere derived from whistler data, J. Atmos. Terr. Phys. **14**, 185.

Cain, J. C. and R. E. Sweeney: Magnetic field mapping of the inner magnetospher, J. geophys. Res. **75**, 4360 (1970).

Ohtsu, J.: Law latitude nose whistlers, Proc. Res. Inst. Atmospherics, Nagoya Univ. **14**, 15 (1967).

Tanaka, Y.: Private communication.